The International Journal of Advanced Manufacturing Technology (2019) 103:985–995
https://doi.org/10.1007/s00170-019-03408-8

ORIGINAL ARTICLE

Experimental determination of the viscoelastic parameters of K-BKZ model and the influence of temperature field on the thickness distribution of ABS thermoforming

Jemyung Cha[1] · Moonjeong Kim[1] · Dongguen Park[2] · Jeung Sang Go[1]

Received: 17 September 2018 / Accepted: 29 January 2019 / Published online: 28 March 2019

Abstract
This study investigated an influence of the temperature field on thickness distribution of thermoformed products using complex and high-aspect-ratio mold. The optimum temperature field was obtained to achieve a more uniform thickness distribution in the thermoformed products by using finite element simulation. The material properties of acrylonitrile-butadiene-styrene (ABS) polymer sheet were obtained by two rheological measurement tests. The linear viscoelastic properties, such as the storage modulus and loss modulus, were measured by a small amplitude oscillatory shear (SAOS) test for wide ranges of frequency and temperature. The discrete relaxation time and discrete relaxation modulus were obtained by nonlinear regression. The fitting parameters C_1 and C_2 for the WLF model were obtained by curve fitting. The nonlinear viscoelastic property, such as stress relaxation modulus, was measured by a step strain test. The damping function and fitting parameter α of Wagner-Demarmels (WD) model were determined by curve fitting. Then, the Kaye–Bernstein-Kearsley-Zapas (K-BKZ) constitutive equation was utilized to the thermoforming simulation in order to investigate the material behavior of the polymer sheet. The numerical results showed that a more uniform thickness distribution could be achieved with the optimum temperature field of the sheet. The thinnest part of the products was improved by more than 30%.

Keywords Thermoforming · Thickness distribution · Viscoelastic properties · Rheological measurement · K-BKZ constitutive equation · FE simulation · Optimum temperature field

1 Introduction

Thermoforming is a processing technology where a polymer sheet is heated to a forming temperature and formed into a specific shape in a mold by application of mechanical deformation, air pressure, and/or vacuum pressure. Figure 1 shows the thermoforming processes consisting of clamping, heating, pre-stretching, mold moving, vacuuming, and trimming. The sheet is held by a clamping tool in the clamping step (Fig. 1a). The sheet is heated until the desired forming temperature is reached, and the softened sheet begins to sag due to gravity in the heating step (Fig. 1b). Then, air pressure is applied to the sheet to achieve a more uniform thickness in the pre-stretching step (Fig. 1c). The mold is moved to the sheet (Fig. 1d), and the sheet contacts with the mold by the vacuum pressure in the forming step (Fig. 1e). Finally, the unnecessary areas of the sheet are trimmed after sufficient cooling and hardening (Fig. 1f).

Thermoforming has advantages, such as an ability to fabricate complex and large shaped products, a low cost for tooling, and the use of various polymer materials. Moreover, the process is highly automated for a mass production. However, thermoforming also has disadvantages, such as a limitation of product shape and thickness variation. Especially, the wall thickness of thermoformed products is important from the point of view in quality and cost. The sheet experiences large deformation, and the local thinning can occur resulting in product failure. Using thicker sheets to prevent thin areas of the products causes increase in cost. Therefore, investigation of the influence of the temperature on thickness distribution of thermoformed products is important.

✉ Jeung Sang Go
micros@pusan.ac.kr

[1] School of Mechanical Engineering, Pusan National University, 2, Busandaehak-ro 63beon-gil, Geumjeong-gu, Busan 46241, Republic of Korea

[2] Department of Advanced Materials and Parts of Transportation Systems, Pusan National University, 2, Busandaehak-ro 63beon-gil, Geumjeong-gu, Busan 46241, Republic of Korea

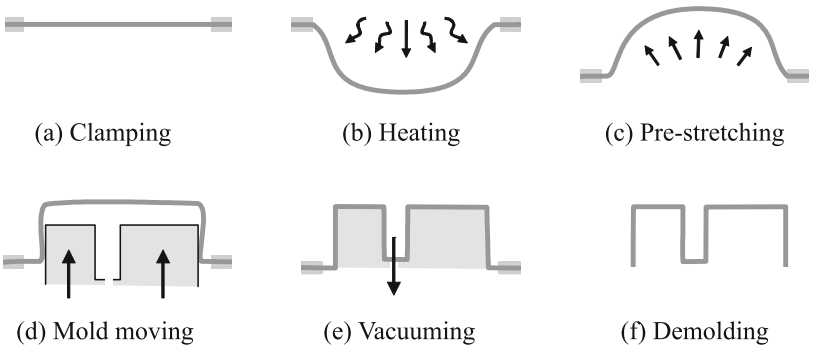

Fig. 1 Thermoforming processes consisting of clamping, heating, pre-stretching, mold moving, vacuuming, and demolding

Thermoforming applications can be categorized according to the thickness of the product. Packaging containers with a thickness of less than 1 mm, such as food, beverages, medical drugs, and semiconductors, are called as thin-gauge thermoformed products. High-durability products with wall thickness range from 1 to 10 mm, such as housings for electrical appliances, automotive parts, yachts, and interior liners, are considered heavy-gauge thermoformed products. They have a wider range of thickness distribution than thin-gauge thermoformed products. Thicker sheets can be used to prevent from excessive thinning. However, the cost of the raw material and the time for heating and cooling down also can be increased. For example, refrigerator inner liners are typical heavy-gauge thermoformed products. They have a complex-shaped mold and a high drawing ratio, resulting in a larger thickness distribution. High-quality thermoforming can be achieved by controlling temperature field on the sheet. So, it is necessary to investigate the influence of temperature on the thickness distribution of the thermoformed products.

Understanding the behavior of polymer materials and property measurement under specific processing conditions is necessary to improve thermoforming performance, such as thickness distribution of the thermoformed products. Over the past few decades, many studies have been devoted to investigate how materials behave under thermoforming conditions, such as range of temperature, strain, and strain rates. Also, finite element simulations have been used to obtain a better thickness distribution of thermoformed products. Nam et al. [1] conducted the simulation of the thermoforming process using a hyperelastic Mooney-Rivlin model. Hot tensile tests with ABS material at high speed were carried out to obtain the Mooney-Rivlin material parameters. They showed that the numerical results using the hyperelastic constitutive model were in a good agreement with the experimental results. They emphasized the sheet temperature field should be considered for a more reliable simulation. Nam and Lee [2] investigated the thermoforming simulation of the refrigerator inner liners made of ABS material. To characterize material behavior, hot tensile and dynamic oscillatory shear tests were performed at various temperatures. The thickness distribution from simulation results was compared with experimental data. It showed that the hyperelastic constitutive model can predict the deformation behavior of the sheet. Sala et al. [3] simulated thermoforming process of the refrigerator inner liners made of high-impact polystyrene (HIPS) material. The G'Sell nonlinear viscoelastic constitutive equation was adopted in the simulation, and the rheological properties of HIPS materials were measured at the range of thermoforming temperature. Understanding the temperature-dependent rheological properties of materials is important to minimize the thickness distribution. Lee et al. [4] studied the effects of rheological properties of ABS sheet and process parameters, such as friction coefficient, heat transfer coefficient, and sheet and mold temperatures on the thickness distribution of the refrigerator inner liners. The SAOS test was performed to determine linear viscoelastic spectra in the frequency range from 10^{-2} to 10^{2} s^{-1} and in the temperature range from 140 to 200 °C. The shear stress growth coefficient was measured from the start-up of steady shear in the shear rate range from 10^{-3} to 10^{1} s^{-1} at 170 °C. The K-BKZ-type single integral nonlinear viscoelastic constitutive model with the measured properties was used in the commercial thermoforming software to describe viscoelastic behavior and large deformation. They reported that rheological properties and the friction coefficient played an important role in determining thermoforming performance compared with other process parameters, such as sheet and mold temperature. Lee et al. [5] performed thermoforming simulation of the refrigerator inner liners. They observed that a small temperature difference on the sheet significantly influences on the local thickness distribution, since it greatly affects the bubble shape in the pre-stretching step. These previous studies focused in selecting appropriate constitutive equations to predict material behavior in thermoforming using numerical simulation and to measure the rheological properties of polymer materials in various conditions, such as range of temperature, strain, and strain rates.

Several works have shown that the thickness distribution of products depends on various process parameters, such as the types of polymer materials, temperature field, heating time, applied pressure, surface friction, material properties, and clamping shape in detail. Ayhan and Zhang [6] studied the effects of process parameters, such

as forming temperature, forming air pressure, and heating time. The wall thickness distribution was examined for food containers made of multilayered material by plug-assisted thermoforming. The thickness distribution of the product was varied with the process parameters, and the optimum parameters were presented. Morales et al. [7] studied the effect of the friction coefficient on temperature in plug-assisted thermoforming process. It was found that the friction coefficient of the sheet varying with temperature greatly influences the thickness distribution. Erdogan and Eksi [8] investigated the effect of circular and rectangular clamping tools to the thickness distribution. The side areas and bottom areas of the thermoformed products are significantly affected by the geometry of the clamping tool. Azdast et al. [9] studied a combination processes, such as free-forming and plug-assisted thermoforming for uniform wall thickness distribution of a hemispherical transparent PMMA sheet. Wang and Nied [10] examined optimization method with finite element simulation to obtain a desired final thickness distribution for simple cylindrical geometry. Nonuniform initial temperatures were obtained by iterative calculations for the desired thickness distribution of the thermoformed products made of ABS material. Wang et al. [11] proposed a new material model based on the uniaxial tensile properties. Meissner-type rheometer was used to measure ABS material to take account for strain hardening, strain rate hardening, and temperature change. Numerical results are compared with experimental results for a simple rectangular cup. Lau et al. [12] studied sagging behavior of different materials, such as polypropylene and ABS used for thermoforming. The dynamic shear test was conducted to measure viscoelastic properties, such as the storage modulus, loss modulus, and complex viscosity. The higher the storage modulus and complex viscosity of the materials showed the greater the sagging resistance. Baek et al. [13] focused calculation of sheet sag using the commercial finite element software. Experimental results were compared with numerical results for HIPS sheets. The amount of sheet sag using isothermal theory was 14 times larger than nonisothermal condition. Wiesche [14] examined thermoforming processes using numerical simulation for an industrial fuel tank, which has complex geometry. The effect of temperature-dependent properties on thickness distribution was investigated. Crystallinity of the materials was discussed in terms of solidification rates. Dong et al. [15] performed the numerical simulation for acrylic sheet using commercial finite element software. Because of the high stretching close to vertical wall areas, a numerical technique of automatic selective mesh refinement was used. Ghobadnam et al. [16] investigated thermoforming parameters, such as heating, vacuum pressure, and mold geometry on the thickness distribution. Increase in the heating time was important to achieve more uniform thickness distribution when using the female mold. However, decrease in heating time was needed for the male mold. Leite et al. [17] studied the effect of thermoforming parameters by using artificial neural network models. The heating time and heating power were the important factors for uniform thickness distribution.

From previous studies, it is clear that the thickness distribution of thermoformed products is greatly influenced by the temperature field and temperature-dependent parameters. In this work, the influence of the temperature on thickness distribution of thermoformed products was investigated. The ABS polymer sheet was characterized by rheological measurements, such as the SAOS test and the step strain test. The linear properties, such as a storage modulus and a loss modulus, were measured by the SAOS test, and the discrete relaxation spectra and Williams-Landel-Ferry (WLF) coefficients were determined by nonlinear regression. The nonlinear stress relaxation modulus was measured over a wide range of strain by the step strain test. The damping function and the fitting parameter α of the WD model were obtained and implemented into the K-BKZ constitutive equation to predict the nonlinear viscoelastic behavior of the ABS polymer under large deformation. Numerical simulations were conducted to investigate influence of temperature field for more uniform thickness distribution of thermoformed products. The flow chart for the research is shown in Fig. 2.

2 Viscoelastic behavior in thermoforming

Polymers are viscoelastic materials, which have both viscous and elastic components. Their response to an applied stress or strain depends on the experimental time scale, and the resulting relationship between stress and strain may be linear or nonlinear. Linear viscoelastic materials exhibit the linear relationship between its stress and strain at a given time, and the material properties remain constant. However, if the strain or strain rate is large enough, considerable nonlinearity can be found and the properties are no longer constant. Polymer sheet experiences various deformations over time at each thermoforming step. The sheet of elevated temperature is deflected by gravity in the heating step, and its deformation rate is relatively lower than in the other step. In the pre-stretching step, the sheet deforms more rapidly by air and/or vacuum pressure, which is called bubble inflation. Then, it undergoes fast deformation by contact with the mold and vacuum pressure in the forming step. These behaviors greatly affect both viscoelastic properties and the thickness distribution of thermoformed products. Therefore, it is necessary to measure the viscoelastic properties of polymer materials under various conditions, such as strain, strain rate, and temperature in thermoforming.

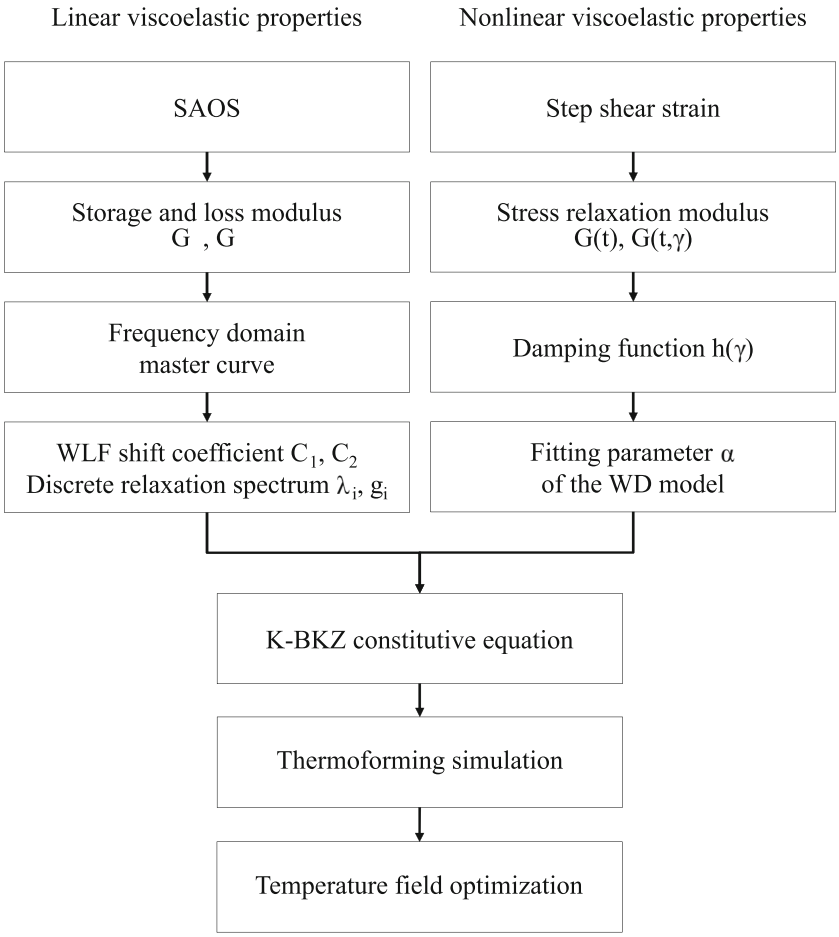

Fig. 2 The flow chart for the research

3 The rheological measurements

Two rheological experiments were carried out to measure the viscoelastic properties by using shear-strain-controlled rotational rheometer over a wide range of strain, strain rate, and temperature from the linear viscoelasticity to the nonlinear viscoelasticity region. Linear viscoelastic properties, such as a storage and loss modulus, can be measured by the SAOS test. The nonlinear viscoelastic property, such as stress relaxation under large strain, can be obtained by the step strain test.

The measurement setup using the rotational rheometer with a parallel plate geometry (ARES-G2, TA instruments) is described in Fig. 3. Thirty samples were prepared from the extruded ABS (M_w = 206,500) sheet produced by LG Chem Ltd., and the dimensions were 13 mm in diameter and 3.4 mm in thickness. The samples were stored in the humidity chamber (ES-80TH, Envtech) for 120 min to remove the effect of moisture. After loading the sample into the parallel plates, nitrogen gas was filled to reduce the oxidization of the molten polymer at high temperatures.

The SAOS test measures stress or strain as a function of frequency by applying sinusoidal stress or strain to characterize the linear viscoelastic properties of the materials. The storage modulus (G') and loss modulus (G'') are obtained as a function of frequency (ω). The G' and G'' were measured for a shear strain of 0.5% by applying the angular frequency in the range between 10^{-1} and 10^{2} rad/s. The temperature was changed from 130 to 220 °C with an ascending temperature

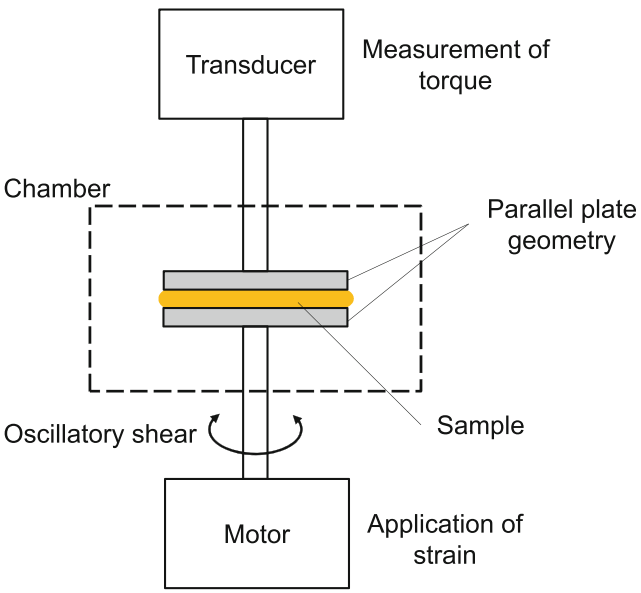

Fig. 3 The measurement setup using the rotational rheometer with a parallel plate geometry

rate of 2 °C/min to investigate the temperature dependence on the linear viscoelastic properties.

Linear viscoelasticity is mainly affected by the polymer structure, such as molecular weight, molecular weight distribution, branch, and entanglement. For example, the entanglement increases as the length of polymer chains increases. As a result, the mobility of the polymer chains is decreased, and the relaxation time is increased. The linear viscoelastic behavior can be characterized by several relaxation times as described in the generalized Maxwell model. The relaxation spectra, such as the discrete relaxation time and discrete relaxation modulus, can be obtained from the dynamic modulus of $G'(\omega)$ and $G''(\omega)$. The N sets of the discrete relaxation time λ_i and the discrete relaxation modulus g_i can be determined by nonlinear regression using following expression

$$G'(\omega) = \sum_{i=1}^{N} \frac{g_i \omega^2 \lambda_i^2}{1+\omega^2\lambda_i^2}, G''(\omega) = \sum_{i=1}^{N} \frac{g_i \omega \lambda_i}{1+\omega^2\lambda_i^2} \quad (1)$$

where λ_i is the discrete relaxation time, g_i is the discrete relaxation modulus, and N is the number of the Maxwell models.

The linear master curve was generated to cover the behavior in wider range of frequency. The $G'(\omega)$ and $G''(\omega)$ were shifted and superposed based on the time-temperature superposition principle at the reference temperature of 170 °C by a horizontal factor of a_T. The discrete relaxation spectra, such as λ_i and g_i, were calculated from the linear master curve of the $G'(\omega)$ and $G''(\omega)$. Figure 4 shows a good agreement between the experimental response displayed with unfilled circles and the estimated response with the discrete relaxation spectra displayed with dotted lines. The eight sets of parameters of the discrete relaxation spectra were given in Table 1.

Temperature dependence of the materials can be considered with the WLF model as follows

$$\log(a_T) = \frac{-C_1(T-T_r)}{C_2+(T-T_r)} \quad (2)$$

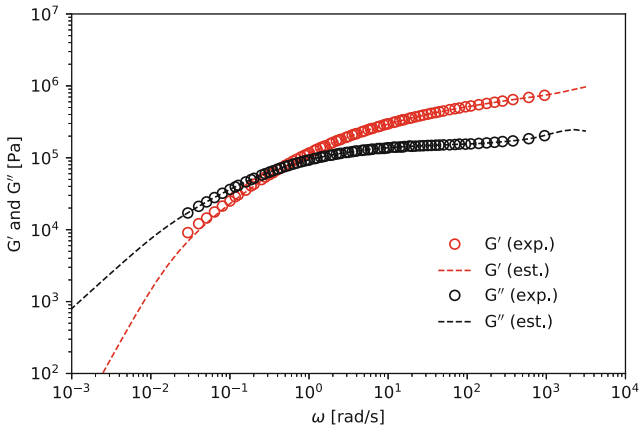

Fig. 4 Good agreement between the experimental response displayed with unfilled circles and the estimated response with the discrete relaxation spectra displayed with dotted lines

Table 1 The discrete relaxation time and discrete relaxation modulus for the ABS polymer at reference temperature of 170 °C

Relaxation time (s)	Modulus (Pa)
8.52×10^{-5}	1.61×10^{6}
1.42×10^{-3}	2.80×10^{5}
1.30×10^{-2}	2.01×10^{5}
9.12×10^{-2}	1.86×10^{5}
5.74×10^{-1}	1.62×10^{5}
3.31×10^{0}	1.03×10^{5}
1.76×10^{1}	4.23×10^{4}
1.31×10^{2}	1.03×10^{4}

where a_T is the horizontal shift factor, T is the temperature, T_r is the reference temperature chosen to generate the master curve, and C_1 and C_2 are the fitting parameters.

The horizontal shift factor a_T means the ratio of relaxation times at one temperature T to the reference temperature T_r. The experimentally obtained shift factor was fitted to the WLF model, and the fitting parameters $C_1 = 5.8$ and $C_2 = 120.8$ K were determined by curve fitting at the reference temperature of 170 °C. They have good agreement between the experimental data and the WLF model as seen in Fig. 5.

The behavior of the polymer materials is linear when strain is sufficiently small and slow. The nonlinear behavior, however, appears as strain increases. Characterization of nonlinear viscoelasticity is necessary to accurately predict the behavior of polymer materials, which undergo large strain and high strain rates in thermoforming. To measure the nonlinear stress relaxation, the step strain test was carried out. By imposing a step-wise shear strain ranging from $\gamma = 0.16$ to $\gamma = 6.28$ at the reference temperature of 170 °C on the ABS sample, the burst stress was relaxed with time. Then, the nonlinear stress relaxation modulus was obtained.

As shown in Fig. 6a, the linear stress relaxation modulus $G(t)$ at $\gamma = 0.16$ and $\gamma = 0.25$ is almost identical meaning that the critical strain γ_c is 0.25. The $G(t)$ at small strain is dependent on time only. Over γ_c, the stress relaxation modulus

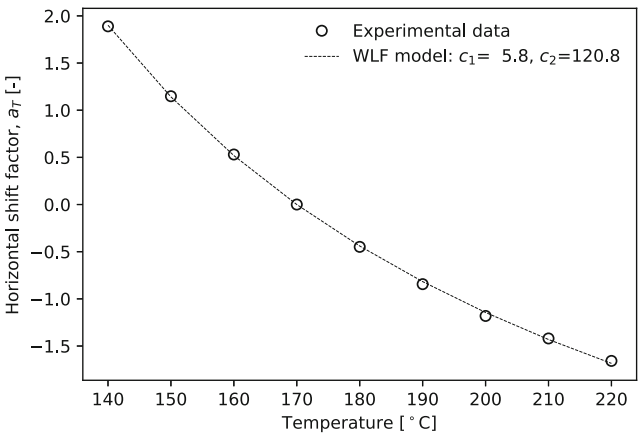

Fig. 5 Good agreement between the experimental data and the WLF model

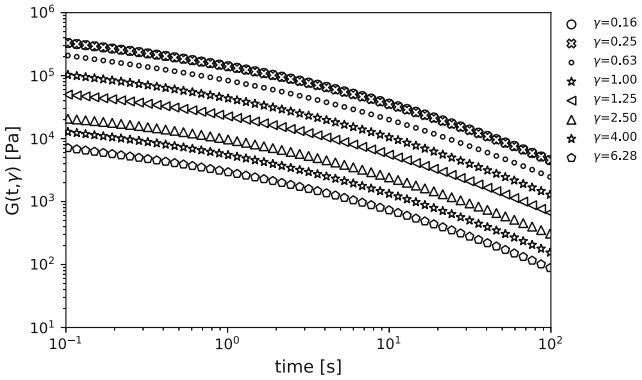

Fig. 6 The linear stress relaxation modulus

decreases as the strain increases, which means that the relaxation modulus $G(t,\gamma)$ is not linear any longer and it is dependent on both time and strain. The time-strain separability was observed for shear relaxation of the ABS polymer.

The damping function is used to express deviation from linear to nonlinear viscoelastic behavior of the material. It has value between one and zero. The material exhibits a linear viscoelastic behavior when the damping function is one, and the materials behavior becomes nonlinear as the damping function approaches to zero. It can be determined by the relationship between the linear and nonlinear relaxation modulus as written in Eq. (3)

$$h(\gamma) = \frac{G(t)}{G(t,\gamma)} \tag{3}$$

where $G(t)$ is the linear stress relaxation modulus, $G(t,\gamma)$ is the nonlinear stress relaxation modulus, and $h(\gamma)$ is the damping function.

$G(t,\gamma)$ was shifted up and superposed to $G(t)$ to obtain damping function $h(\gamma)$, as shown in Fig. 6b. Then, $h(\gamma)$ was calculated as described in Eq. (3). As given in Table 2, three models of damping function, such as the Papanastasiou-Scriven-Macosko (PSM), the Wagner model, and the WD model, can be selected to describe the nonlinear behavior of the ABS polymer. Because the PSM and the WD models are identical for the shear deformation, the PSM model was not considered here. Curve fitting was performed on the experimental data to obtain fitting parameter α of the Wagner model and the WD model. The results are shown in Fig. 7. When the strain is small enough, they predict the behavior similar to the experimental data. As strain increases, however, the WD model shows better prediction than the Wagner model. The sum of the square error (SSE) of WD models was 0.002, and the SSE of the Wagner model is 0.008. The damping function of sigmoidal form has better prediction with respect to experimental data than exponential form.

Table 2 Three models of the damping function for shear deformation where the α is the fitting parameter of each model

Model	Equation
PSM model	$h(\gamma) = \alpha \,/\, (\alpha + \gamma^2)$
Wagner model	$h(\gamma) = \exp(-\alpha\gamma)$
WD model	$h(\gamma) = 1 \,/\, (1 + \alpha^{-1}\gamma^2)$

4 Constitutive models

The polymer materials exhibit nonlinear viscoelastic behavior because they are subjected to large strain and high rate of strain. It is important to consider the time-dependent and strain-dependent of the viscoelastic materials to investigate the nonlinear behavior of the polymer materials in thermoforming. In this work, K-BKZ type of single integral constitutive equation is utilized to predict the behavior of polymer material [18, 19]. The Lodge network model is recognized as the most basic viscoelastic integral constitutive equation to describe nonlinear behavior of polymer materials. The Lodge model with multiple relaxation processes is as follows [20]

$$\tau(t) = \int_{-\infty}^{t} m\left(t-t'\right)\cdot B\left(t,t'\right)dt' \tag{4}$$

where $m(t,t')$ is the memory function, which is time derivative of relaxation modulus, and $B(t,t')$ is the Finger strain tensor.

The Lodge model can only explain linear viscoelastic behavior with time-dependent memory function, which is expressed as the sum of exponentially fading memory terms

$$m\left(t-t'\right) = \sum_{i=1}^{N} g_i \exp\left(-\frac{t-t'}{\lambda_i}\right) \tag{5}$$

where g_i are the relaxation moduli and λ_i are relaxation times, and they can be determined experimentally as in the SAOS test.

It cannot accurately predict nonlinear viscoelastic behavior of the materials, since the memory function under large deformation depends both on time and strain. Wagner presented the idea of separability of the memory function by factoring it into

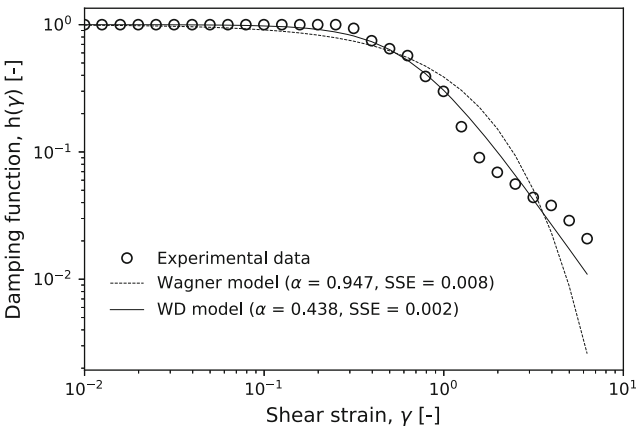

Fig. 7 Curve fitting was performed on the experimental data to obtain fitting parameter of the Wagner model and the WD model

time-dependent term and strain-dependent term based on the Lodge model [21]. The memory function can be expressed as the product of the time-dependent linear function and the strain-dependent nonlinear function.

$$m\left[\left(t-t'\right),I,II\right]=m\left(t-t'\right)h(I,II) \tag{6}$$

where $m(t,t')$ is the memory function in linear viscoelasticity, and $h(I,II)$ is the damping function in nonlinear viscoelasticity.

The K-BKZ-type nonlinear viscoelastic constitutive model with the damping function can be written as

$$\tau(t)=\int_{-\infty}^{t}m\left(t-t'\right)\cdot h(I,II)\cdot B\left(t,t'\right)dt'. \tag{7}$$

This time-strain separable model proposed by Wagner is a simplified version of the K-BKZ model. Under shear deformation, the models can be expressed with the damping function $h(\gamma)$ as follows

$$\tau(t)=\int_{-\infty}^{t}m\left(t-t'\right)\cdot h(\gamma)\gamma\left(t,t'\right)dt'. \tag{8}$$

The WD model was chosen for the damping function in this work because it showed better prediction than the Wagner model, as shown in Fig. 7.

5 Numerical simulation of thickness distribution of the thermoformed products

The three-dimensional finite element simulation with the K-BKZ constitutive model was conducted to examine the behavior of the ABS polymer sheet in thermoforming. Then, the influence of temperature field on thickness distribution of thermoformed products and optimum temperature field was investigated. Thermoforming consists of the following three main steps: (i) heating, in which the sheet is heated until the desired forming temperature is reached; (ii) pre-stretching, in which air pressure is applied to the sheet to obtain more uniform thickness and the sheet is inflated like bubble; and (iii) forming, in which the inflated sheet is deformed by the mold and vacuum pressure is applied to the sheet. The commercial finite element software (T-SIM, version 4.8) was used to investigate the behavior of polymer sheet in these three steps of thermoforming. This work focused on examining how the thickness distribution of the thermoformed products is affected by temperature.

The width, depth, and height of the thermoformed refrigerator inner case were 840 mm × 740 mm × 1620 mm. The inner case consisted of an upper compartment with a height of 820 mm and a lower compartment with a height of 760 mm, and there is a narrow gap of 40 mm between them, as shown in Fig. 8. A significant thickness variation can occur due to geometric characteristics of the deep drawing mold. The sheet is highly stretched by the mold in the forming step. The top area of the sheet is cooled as soon as it contacts with the mold, and the stretching is stopped. Its thickness has no more changes, and it is thicker than the side wall or edge area. The side wall of the polymer sheet experiences considerable strain resulting in greater thickness variation in the product. Since the edge area is clamped, there is no significant change in thickness.

The FE model for the thermoforming simulation is depicted in Fig. 9. The polymer was approximated with a membrane. It was meshed with the triangular finite elements of 50,000 through the convergence test for the number of elements. The thermoforming mold was modeled as rigid

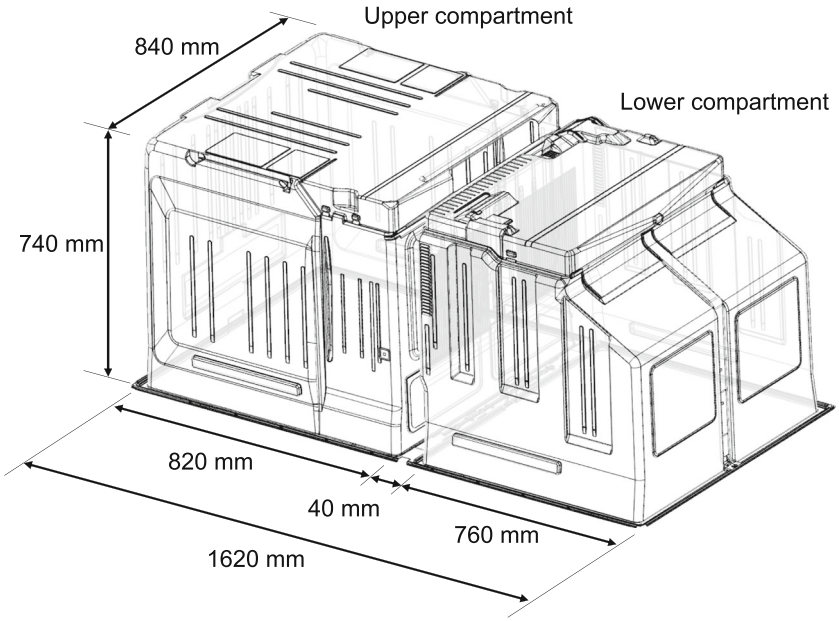

Fig. 8 The inner case is consisted of an upper compartment with a height of 820 mm and a lower compartment with a height of 760 mm

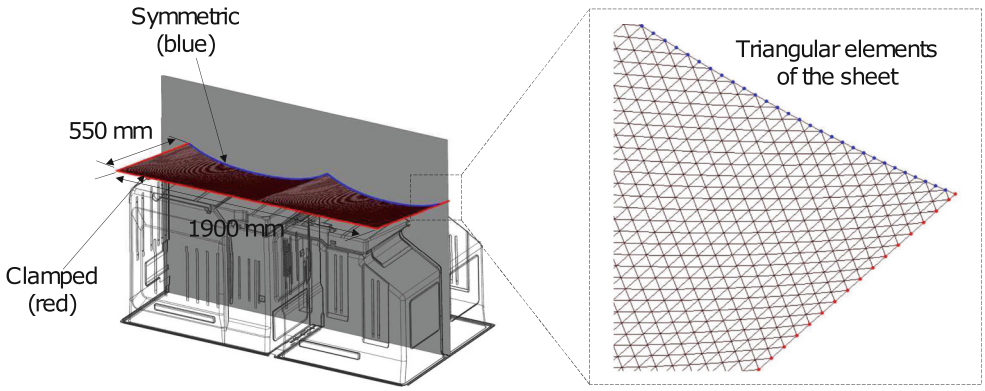

Fig. 9 The FE model for the thermoforming simulation

body. The boundary condition along the edge of the sheet was assumed zero wall velocity. By considering the symmetric shape of the inner case, the half was simulated for efficient computation. Also, the boundary condition of velocity normal to the cross-section was set to be zero. The initial temperature field of the polymer sheet and the mold temperature were 170 and 60 °C, respectively. The contact between the polymer sheet and the mold surface was considered as the Coulomb friction. The friction coefficient was assumed to be 1.5 at 170 °C [3]. The coefficient of convection heat transfer was 8 W/m^2 k, which was applied to the sheet surface.

A transient simulation was conducted for the process parameters, such as the differential pressure profile and the changing mold position with time, as shown in Fig. 10. Positive differential pressure was applied on the sheet to inflate during the pre-stretching step from 0 to 5 s. Then, negative differential pressure was applied on the sheet to contact the mold surface in the forming step. The mold was stayed at the initial position until 5 s, and it moved to its maximum position until 6 s. Then, it stopped until the process was completed.

Finally, the K-BKZ-type viscoelastic constitutive model with the damping function was adopted to examine the nonlinear behavior of the polymer materials in thermoforming. In the thermoforming simulation, the used material properties were the same with those obtained from the rheological measurements of the relaxation spectra listed in Table 1, WLF shift

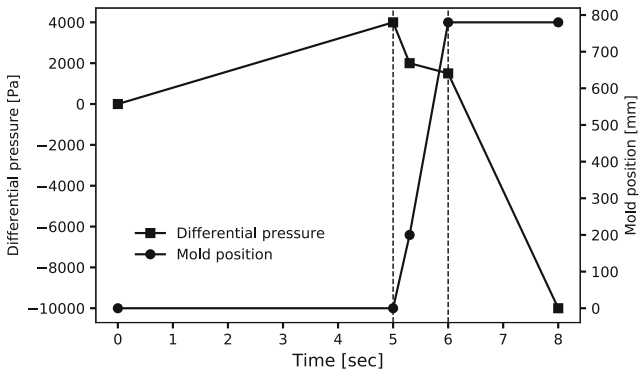

Fig. 10 A transient simulation conducted for the process parameters

model ($C_1 = 5.8$ and $C_2 = 120.8$ K) shown in Fig. 5, and damping function ($\alpha = 0.438$ for WD model) in Fig. 7.

6 Results and discussion

Figure 11 shows four stages of numerical results. At the beginning of the simulation, pressure inside the chamber increases linearly with the application of the air flow. The bubble is inflated with applied air pressure, and it contacts with the mold, as shown in Fig. 11a. The bubble grows until the air pressure is not enough to inflate the bubble. The thinness wall area is between the upper and lower compartments, as shown in Fig. 11b. The mold is moved upwards, and the vacuum pressure is applied to the sheet to form the same shape of the mold in Fig. 11c. Finally, the sufficiently cooled and hardened product is obtained, as shown in Fig. 11d.

Nonuniform thickness distribution was observed at the end of thermoforming process. Thick areas in some location were found, but thin areas in other location also were found. It is possible to obtain more uniform thickness distribution with appropriate temperature field instead of using the thick sheet to prevent to excessive thinning. The effect of the temperature on the thickness distribution of thermoformed products was numerically investigated. Several runs of numerical simulations are required to examine the temperature effect on the thickness distribution. The new temperature field will be calculated based on the obtained thickness distribution. The temperature of each node with a greater thickness than the desired thickness should be increased. Conversely, the new temperature of each node with a lower thickness should be decreased as follows

$$T^{\text{new}} = T^{\text{prev}} + C(T - T^{\text{prev}}) \tag{9}$$

where T^{new} is the new solution, T^{prev} is the previous solution, C is under relaxation factor, and T can be obtained by following function

$$f(T) = f(T^{\text{prev}}) \cdot h^{\text{desired}} / h^{\text{current}} \tag{10}$$

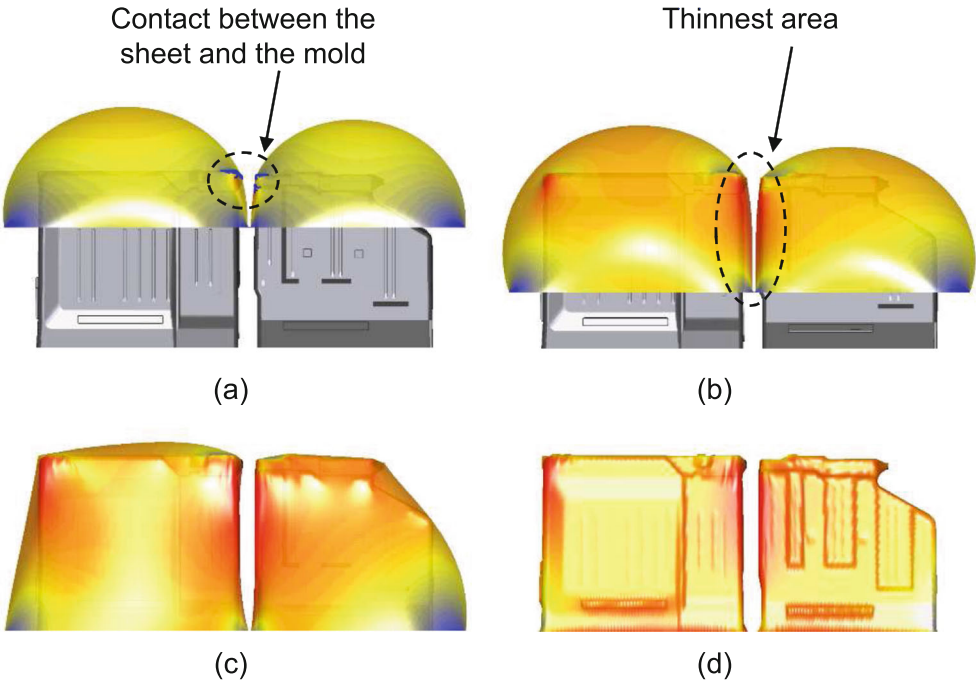

Fig. 11 The four stages of numerical results

where h^{desired} is the desired thickness, h^{current} is the current thickness, and $f(T)$ is the dependency law as a function of temperature.

Several runs of the simulation are required to improve thickness distribution of the product by change of the temperature at each node. A new temperature field is calculated at each run of the simulation. It is imposed on the next run of the simulation based on the previous temperature solution as described in Eqs. (9) and (10). For example, uniform temperature field of 170 °C was applied to the sheet as an initial estimation. Then, the temperature range, such as maximum temperature of 185 °C and the minimum temperature of 170 °C, was applied to the next run to search the appropriate temperature field. These values should be specified in consideration of realistic conditions.

Figure 12 shows the contours of thickness distribution and temperature field in each simulation run. Figure 12a shows the first run #1 with uniform temperature field of 170 °C as the initial estimation. The minimum thickness area is between the upper and lower compartments as is also described in Fig. 11b. In the second run #2, the minimum thickness at the same area became thicker, such as red color changed to orange color, as shown in Fig. 12b. The optimized temperature field to improve thickness distribution was obtained at the final run #6, as shown in Fig. 12c.

The optimized temperature field of the final run # 6 is shown in Fig. 13 as a two-dimensional matrix. The maximum temperature was imposed at the sidewalls and corner walls to further stretch the sheet, while the minimum temperature was imposed at the narrow gap between the upper and lower compartments to reduce stretching. Several solutions can be obtained depending on the process parameters, such as mold geometry, mold speed, pressure profile, and material properties of the sheet.

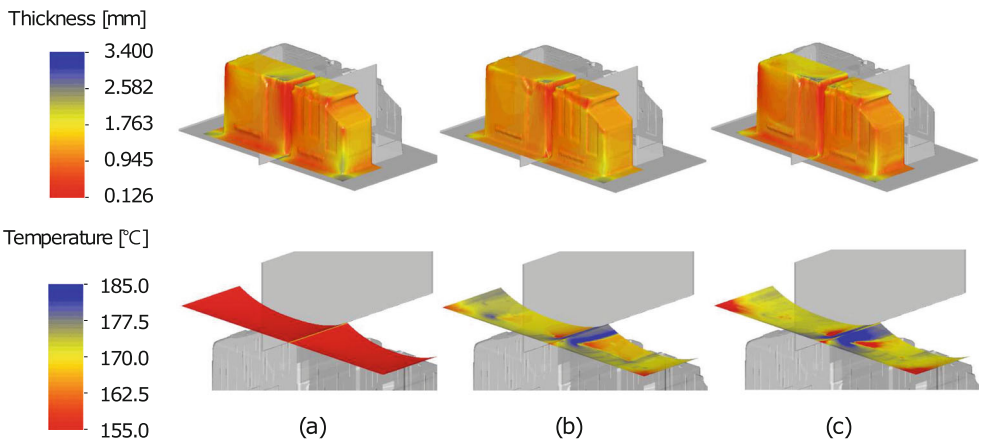

Fig. 12 The contours of thickness distribution and temperature field in each simulation run

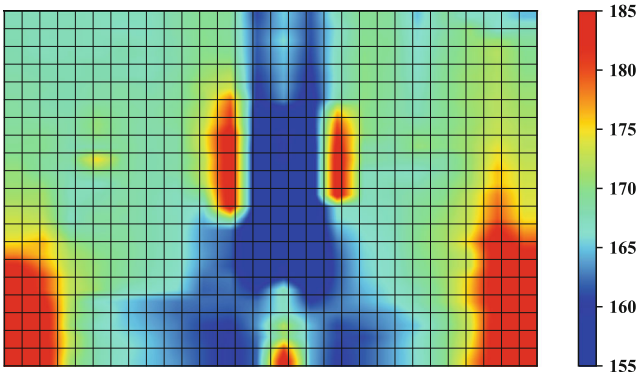

Fig. 13 The optimized temperature field of the final run #6

The thickness in the upper compartment and lower compartment and along the symmetric plane was investigated, as shown in Fig. 14. The simulated thickness at the optimized temperature field was compared with that at the uniform temperature filed. Along the line A-A′ in the upper compartment in Fig. 14a, the minimum thickness on the side wall was increased to 31.6%. Also, along the line B-B′ in the lower compartment plotted in Fig. 14b, the minimum thickness was increased to 60.7%. Along the line C-C′ on the symmetric plane in Fig. 14c, the minimum thickness increased to 65.2%. It can be concluded that the optimized temperature field can provide more uniform thickness distribution of the thermoforming polymer products.

For the verification of the FE modeling, the thermoforming was conducted with three ABS plates at the optimized temperature field condition, and the thickness was measured along the symmetric line. Figure 15 compares the thickness distribution obtained from the numerical analysis of the FE model and measured from the three thermoformed products. From the average thickness measured from the three thermoformed products and the numerical thickness along the symmetric line, the standard deviation was determined to be about 0.147 mm for the optimum thickness of 0.77 mm. They show a relatively good agreement, but there is also discrepancy between them. It resulted from the material properties of the polymer plates, process parameters, and so on.

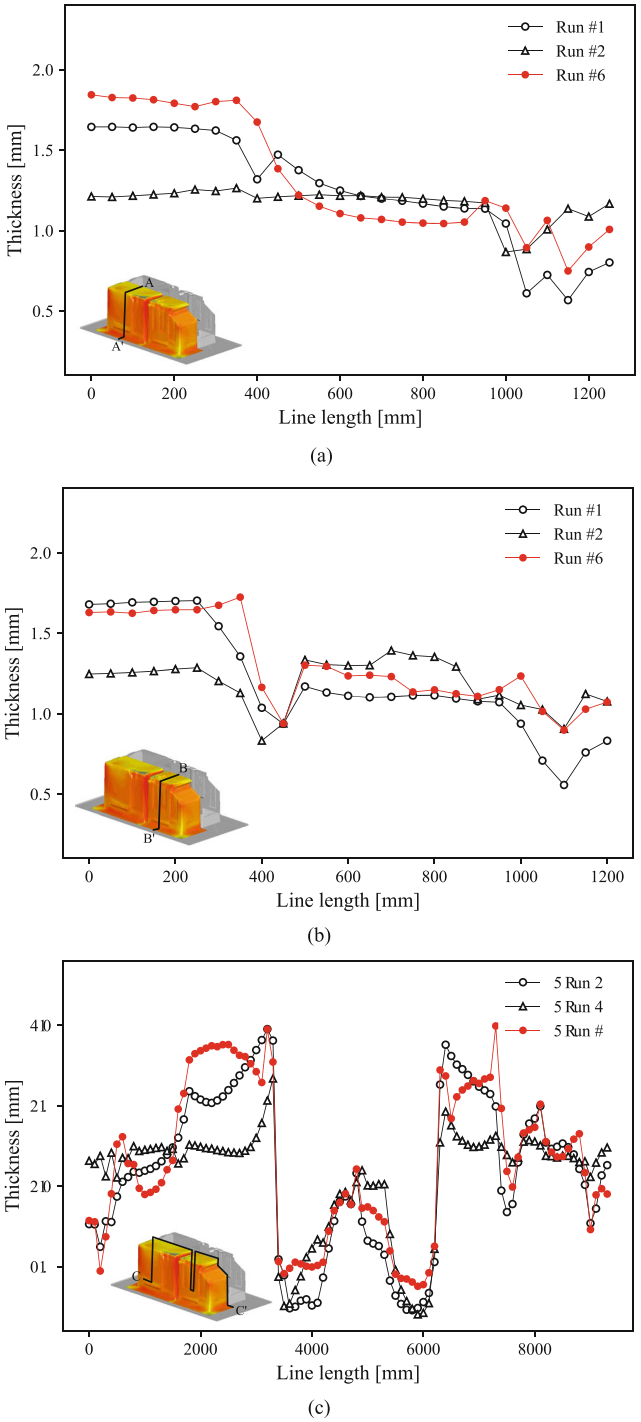

Fig. 14 The thickness in the upper compartment and lower compartment and along the symmetric plane

7 Conclusions

In this work, the thickness distribution of the thermoformed ABS products was improved by optimizing the temperature field. Specifically, to examine the thermoforming behavior of the ABS sheet, the K-BKZ constitutive model was used due to its viscoelastic property at high temperature. The linear and nonlinear viscoelastic properties of the ABS polymer sheet were obtained experimentally by the rheological measurements.

From the SAOS test, the storage modulus and loss modulus for the different conditions of temperature and frequency were measured, respectively. The linear master curve was generated to cover the linear viscoelastic behavior in wider range of frequency. Then, the discrete relaxation spectra were obtained to examine the linear viscoelastic behavior, and the fitting parameters of the WLF model were calculated to describe the temperature dependence of the ABS sheet. The nonlinear stress relaxation

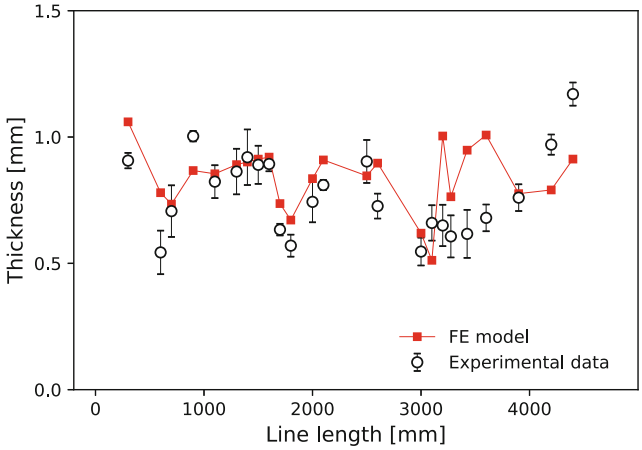

Fig. 15 Comparison the thickness distribution obtained from the numerical analysis of the FE model and measured from the three thermoformed products

modulus was measured from the step strain test, followed by the calculation of the damping function. Finally, the fitting parameter of the WD model was obtained from the damping function to describe the nonlinear viscoelastic behavior. Then, the numerical simulation of the thermoforming of the ABS sheet was conducted with the K-BKZ constitutive model. The thickness distribution of the thermoformed ABS products was improved by optimizing the temperature field situated on the sheet. The minimum thickness of the thermoformed ABS products at the optimized temperature field was improved by more than 30%, compared with that at uniform temperature field.

In manufacturing the thermoformed polymer sheets with the viscoelastic properties due to high temperature, the results and the procedure developed in this work can be applied to the production of refrigerator inner liners. Also, this approach can help to expect the uniform thermoforming of the polymer products with more complex shape and high aspect ratio.

Funding information This work was supported by a 2-Year Research Grant of Pusan National University.

References

1. Nam GJ, Ahn KH, Lee JW (2000) Three-dimensional simulation of thermoforming process and its comparison with experiments. Polym Eng Sci 40:2232–2240
2. Nam GJ, Lee JW (2001) Numerical and experimental studies of 3-dimensional thermoforming process. J Reinf Plast Compos 20: 1182–1190
3. Sala G, Cassago D, Di Landro L (2002) A numerical and experimental approach to optimise sheet stamping technologies: polymers thermoforming. Mater Des 23:21–39
4. Lee JK, Virkler TL, Scott CE (2001) Effects of rheological properties and process parameters on ABS thermoforming. Polym Eng Sci 41:240–261
5. Lee JK, Virkler TL, Scott CE (2001) Influence of initial sheet temperature on ABS thermoforming. Polym Eng Sci 41:1830–1844
6. Ayhan Z, Zhang QH (2000) Wall thickness distribution in thermoformed food containers produced by a Benco aseptic packaging machine. Polym Eng Sci 40:1–10
7. Morales RA, Candal MV, Santana OO, Gordillo A, Salazar R (2014) Effect of the thermoforming process variables on the sheet friction coefficient. Mater Des 53:1097–1103
8. Erdogan ES, Eksi O (2014) Prediction of wall thickness distribution in simple thermoforming moulds. J Mech Eng 60:195–202
9. Azdast T, Doniavi A, Rash Ahmadi S, Amiri E (2013) Numerical and experimental analysis of wall thickness variation of a hemispherical PMMA sheet in thermoforming process. Int J Adv Manuf Technol 64:113–122
10. Wang CH, Nied HF (1999) Temperature optimization for improved thickness control in thermoforming. J Mater Process Manuf Sci 8: 113–126
11. Wang S, Makinouchi A, Tosa T, Kidokoro K, Okamoto M, Kotaka T, Nakagawa T (1999) Numerical simulation of acrylonitrile-butadiene-styrene material's vacuum forming process. J Mater Process Technol 91:219–225
12. Lau HC, Bhattacharya SN, Field GJ (2000) Influence of rheological properties on the sagging of polypropylene and ABS sheet for thermoforming applications. Polym Eng Sci 40:1564–1570
13. Baek HM, Giacomin AJ, Wurz MJ (2014) Sag in commercial thermoforming. AICHE J 60:1529–1535
14. Aus Der Wiesche S (2004) Industrial thermoforming simulation of automotive fuel tanks. Appl Therm Eng 24:2391–2409
15. Dong Y, Lin RJT, Bhattacharyya D (2006) Finite element simulation on thermoforming acrylic sheets using dynamic explicit method. Polym Polym Compos 14:307–328
16. Ghobadnam M, Mosaddegh P, Rezaei Rejani M et al (2014) Numerical and experimental analysis of HIPS sheets in thermoforming process. Int J Adv Manuf Technol 76:1079–1089
17. Leite W, Campos Rubio J, Mata Cabrera F, Carrasco A, Hanafi I (2018) Vacuum thermoforming process: an approach to modeling and optimization using artificial neural networks. Polymers (Basel) 10:143
18. Kaye A (1962) Non-Newtonian flow in incompressible fluids. Aerosp Eng reports, Tech Univ Delft 1–20
19. Bernstein B, Kearsley EA, Zapas LJ (1963) A study of stress relaxation with finite strain. Trans Soc Rheol 7:391–410
20. Lodge AS (1956) A network theory of flow birefringence and stress in concentrated polymer solutions. Trans Faraday Soc 52:120
21. Wagner MH (1976) Analysis of time-dependent non-linear stress-growth data for shear and elongational flow of a low-density branched polyethylene melt. Rheol Acta 15:136–142